Phase behavior and dynamics of a cholesteric liquid crystal

D. Roy,[1] D. Fragiadakis,[1] C. M. Roland,[1] R. Dabrowski,[2] J. Dziaduszek,[2] and S. Urban[3]
[1]*Naval Research Laboratory, Chemistry Division, Code 6120, Washington DC 20375-5342, USA*
[2]*Institute of Chemistry, Military University of Technology, 00-908 Warsaw, Poland*
[3]*Institute of Physics, Jagiellonian University, Krakow, Poland*

(Received 6 January 2014; accepted 30 January 2014; published online 18 February 2014)

The synthesis, equation of state, phase diagram, and dielectric relaxation properties are reported for a new liquid crystal, 4′-butyl-4-(2-methylbutoxy)azoxybenzene (4ABO5*), which exhibits a cholesteric phase at ambient temperature. The steepness of the intermolecular potential was characterized from the thermodynamic potential parameter, $\Gamma = 4.3 \pm 0.1$ and the dynamic scaling exponent, $\gamma = 3.5 \pm 0.2$. The difference between them is similar to that seen previously for nematic and smectic liquid crystals, with the near equivalence of Γ and γ consistent with the near constancy of the relaxation time of 4ABO5* at the cholesteric to isotropic phase transition (i.e., the clearing line). Thus, chirality does not cause deviations from the general relationship between thermodynamics and dynamics in the ordered phase of liquid crystals. The ionic conductivity of 4ABO5* shows strong coupling to the reorientational dynamics. © *2014 AIP Publishing LLC*. [http://dx.doi.org/10.1063/1.4865413]

I. INTRODUCTION

Liquid crystals exhibit simultaneously solid and fluid properties, unusual behavior that makes their dynamics especially interesting.[1] The liquid crystalline state involves arrest of the orientational, and to a lesser extent positional, degrees of freedom, but the absence of three-dimensional order allows mobility.[2,3] Theories of liquid crystals are based generally on anisotropic intermolecular attractions, as in the classic model of Maier and Saupe,[4] or packing considerations and thus repulsive interactions, as in entropy models often deriving from the work of Onsager.[5] The prototypical liquid crystal ordering is the nematic phase, the dynamics of which has received much attention. It has been shown that the relaxation time for the flip-flop motion (rotation of the molecules about their short axes, made possible by fluctuations of the centers of mass) depends only on the product variable of temperature and specific volume:

$$\tau = f(TV^{\gamma}), \tag{1}$$

where f is a function and γ is a material constant.[6–8] This is intriguing because from molecular dynamics simulations (mds) the scaling exponent is seen to be related to the steepness of the intermolecular potential.[9,10] The thermodynamic ratio, Γ (also known as the thermodynamic potential parameter), defined according to[11,12]

$$\Gamma = -(\partial \log T / \log V)_{P_2}, \tag{2}$$

where P_2 is the second rank order parameter, can be evaluated at a phase transition,

$$\Gamma(T_c) = -(\partial \log T_c / \log V_c)_P, \tag{3}$$

implying that the degree of ordering is independent of pressure, P, at a liquid crystal transition. For many nematic and smectic liquid crystals it has been shown that this dynamic scaling exponent γ bears a close approximation to Γ,[6,7,13,14] a result corroborated by recent simulations.[15]

We have pointed out that the equivalence $\Gamma = \gamma$ implies that the relaxation time τ must be constant at a phase transition,[16] although Satoh[15] avers that an order parameter that is invariant at a liquid crystal transition[2] gives the same result. Of course, if τ is a function of P_2, the two interpretations are equivalent. Consistent with simulation results for Lennard-Jones particles[9,10] that show the connection between the magnitude of γ and the slope of the intermolecular repulsive potential, mds of liquid crystals[15] found that Γ was larger for a stronger anisotropic term. (Note that stronger attractive interactions increase the effective slope of the repulsive potential.[17,18])

The studies described above have focused primarily on nematic liquid crystals. In this work we investigate the chiral nematic (cholesteric) liquid crystal, 4′-butyl-4-(2-methylbutoxy)azoxybenzene (4ABO5*). The physical properties of cholesteric liquid crystals are similar to nematic liquid crystals, except the presence of a chiral center results in the director axis assuming a helical form. From calorimetry and PVT measurements we determined $\Gamma = 4.3 \pm 0.1$, and from superposition of dielectric relaxation times measured at high pressures we deduced $\gamma = 3.5 \pm 0.2$. The density scaling for this substance is poorer than usually found for liquids and liquid crystals, although the two exponents are closer in value than found for the only cholesteric liquid previously analyzed, 5*CB,[19,20] for which Γ was about 60% larger than γ. Consistent with the near equivalence of the thermodynamic and dynamic parameters for 4ABO5*, the relaxation time is roughly constant along the clearing line.

II. EXPERIMENTAL

The 4′-butyl-4-(S)-(2-methylbutoxy)azoxybenzene is a mixture of isomers differing by location of the oxygen atom,

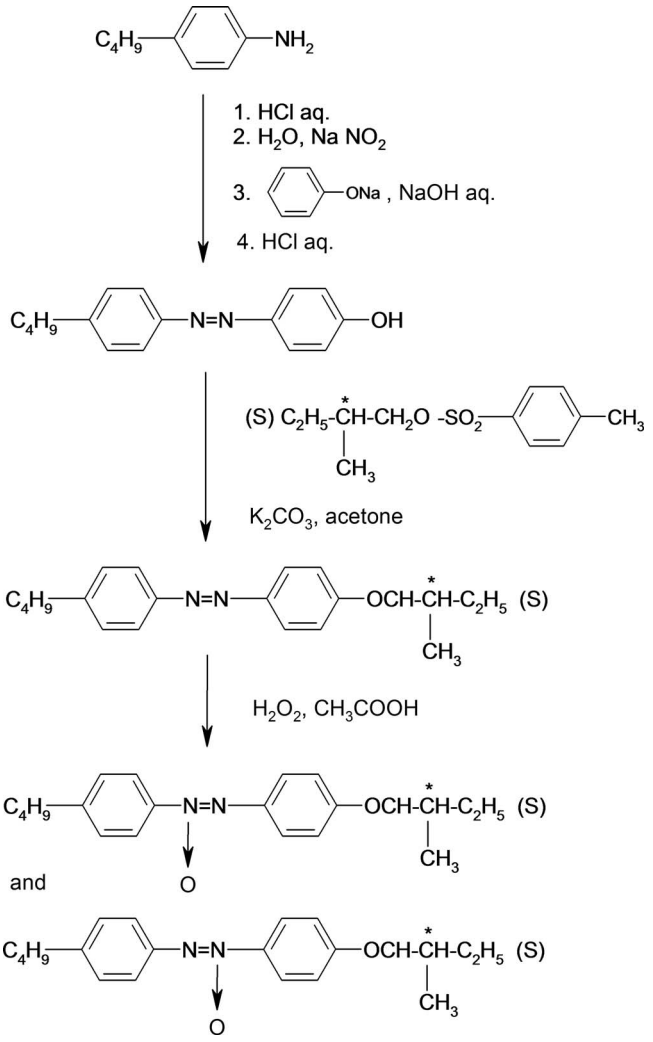

SCHEME 1. Synthesis of 4′-butyl-4-(2-methylbutoxy)azoxybenzene isomers. The chiral center is indicated by the asterisk.

which can be positioned to either side of the azo group. Note that the dipole moment of the isomers differs slightly.[21] The compound was prepared according to the procedure (Scheme 1): 4-butylaniline (Aldrich) was converted to hydrochloride by addition of 5 wt. % of 1.5 mole excess of hydrochlorine acid, followed by stoichiometric addition of an aqueous solution of $NaNO_2$ at 5 °C. Phenol was dissolved in 2.5 mole excess of 5 wt. % NaOH and added quickly to the solution of the diazonium salt. The separated 4′-butyl-4-hydroxyazobenzene was etherified with an acetone solution of 2-methylbutyltoluenosulphonate (prepared from (S)-(-)-2-methylbutanol from Aldrich) in the presence of solid K_2CO_3. The (S)-4′-butyl-4-(2-methylbutyl)azoxybenzene solution, after filtration and removal of acetone, was dissolved in acetic acid, followed by dropwise addition at 80 °C of hydrogen peroxide (30 wt. % solution) until the solution turned yellow. The mixture was poured into water, extracted with CH_2Cl_2, dried over $MgSO_4$, and filtered through silica. After removing of CH_2Cl_2, the compound was recrystallized from methanol.

Dielectric relaxation spectroscopy was carried out using cylindrical electrodes (20 mm diameter) with a 0.1 mm Teflon spacer inserted to maintain constant thickness. Spectra were obtained with a Novocontrol Alpha analyzer at frequencies from 10^{-2} to 10^{6} Hz. For ambient pressure measurements, the temperature was controlled using a Delta Design model 9023 oven. For elevated pressure measurements, the sample capacitor assembly was contained in a Manganin cell (Harwood Engineering) placed in a Tenney Jr. chamber; temperature control was ±0.1 K at the sample. The sample capacitor was protected from contamination by the surrounding medium by flexible seals. The pressure was applied using a hydraulic pump (Enerpac) in combination with a pressure intensifier (Harwood Engineering). Pressures were measured with a Sensotec tensometric transducer (150 kPa resolution) and a Heise pressure gauge (70 kPa accuracy).

Pressure-volume-temperature (PVT) measurements utilized a Gnomix instrument.[22] The change in specific volume was measured during cooling at 0.5°/min at various pressures up to 200 MPa. Differential scanning calorimetry at 0.1 MPa was carried out at 0.5 °/min.

III. RESULTS

A. Thermodynamic transitions

Figure 1 shows the specific volume as a function of temperature for various pressures, measured at a constant (slow) cooling rate. Two phase changes are evident, corresponding to the isotropic–cholesteric and cholesteric–crystalline transitions, at higher and lower temperatures, respectively. Both are first order transitions, yielding discontinuities in the density. Ordering of the isotropic state is associated with a relatively small volume change, $\Delta V_{iso\text{-}ch} = 10^{-3}$ ml/g, barely discernible on the axes-scales necessary to show the crystalline transition. $\Delta V_{iso\text{-}ch}$ decreases only weakly with pressure, $\frac{d\Delta V_{iso-ch}}{dP} \approx -1\,\mu$l/g per GPa. The temperature of the isotropic–cholesteric phase change is invariant to thermal history (e.g., occurring at the same temperature for heating and

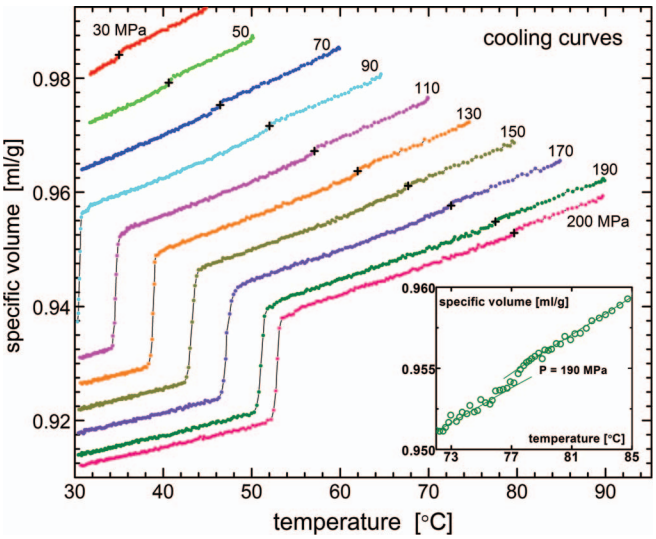

FIG. 1. Specific volume vs. temperature obtained during cooling at each of the indicated pressures. The crosses denote the isotropic–cholesteric transition, which is shown on an expanded scale in the inset for $P = 190$ MPa.

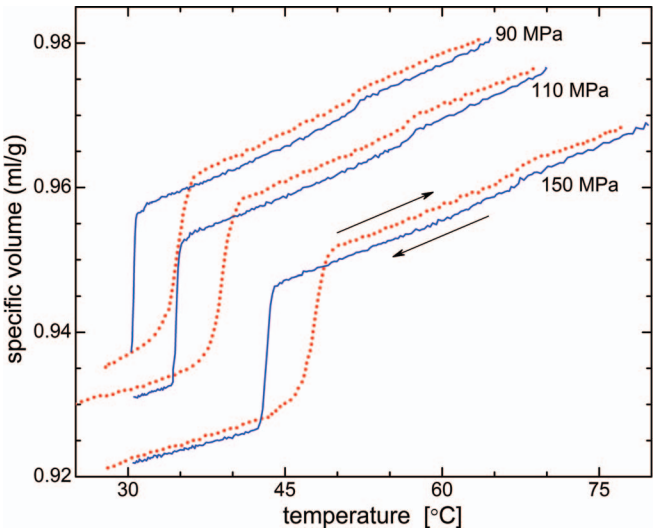

FIG. 2. Representative heating and cooling curves showing supercooling for the cholestric–crystalline phase transition, whereas the isotropic–cholesteric transition is reversible.

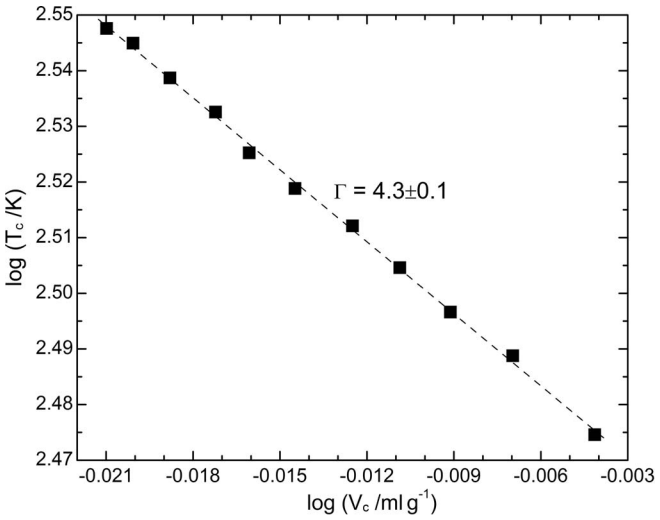

FIG. 4. Temperature and specific volume at the isotropic-cholesteric transition measured at pressures from 30 to 200 MPa. The slope of the double logarithmic plot yields the indicated value of the potential parameter.

cooling as shown in Figure 2), whereas the ordered state can be supercooled, the crystal melting temperature being higher by ∼6° for heating than cooling. These transition temperatures are plotted in Figure 3, which also shows for comparison the calorimetry results for ambient pressure. From the latter the transition enthalpies were determined to be 7.74 and 0.34 kJ/mol for the crystalline to cholesteric and cholesteric to isotropic transitions, respectively.

In Figure 4 the isotropic-cholesteric transition temperature is shown as a function of the specific volume; the double logarithmic plot yields (Eq.(3)) $\Gamma = 4.3 \pm 0.1$. This is in the range of the values of the thermodynamic ratio reported for many other liquid crystals, mostly nematics.

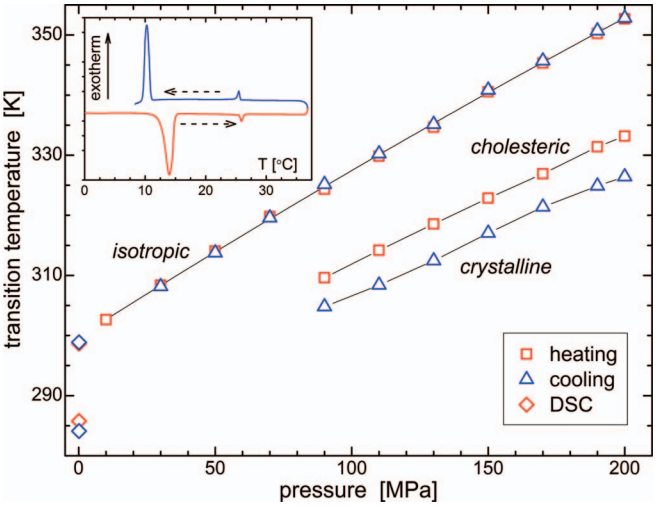

FIG. 3. Transition temperatures determined from volume measurements during heating (squares) and cooling (triangles), along with the ambient pressure results from calorimetry (diamonds). The latter measurements are shown in the inset.

Fitting the Tait equation of state[22] to the PVT data we obtain for the isotropic phase,

$$V_{iso} = 0.971 \exp(8.32 \times 10^{-4} T) \times \left[1 - 0.0894 \ln\left(1 + \frac{P}{186.7 \exp(-0.004T)}\right)\right], \quad (4)$$

and for the cholesteric phase,

$$V_{ch} = 0.970 \exp(8.17 \times 10^{-4} T) \times \left[1 - 0.0789 \ln\left(1 + \frac{P}{164.8 \exp(-0.005T)}\right)\right]. \quad (5)$$

These fits are used to obtain the volume-dependence of the dielectric relaxation times measured as a function of temperature and pressure.

B. Dynamic behavior

There is a relaxation peak in the dielectric spectra for 4ABO5* (Figure 5) due to longitudinal reorientation of the molecules. This peak is readily measured in the cholesteric phase, but above the clearing point, where the structure and motion become isotropic, falls at frequencies ($>10^7$ Hz) beyond the range of our high pressure dielectric capability. As shown in the inset, traversal of the transition is accompanied by a perturbation in the dielectric constant (relative permittivity).

Representative dielectric spectra for various state points within the cholesteric phase are shown in Figure 6. Below about 10 °C 4ABO5* begins to crystallize during the measurement, distorting the spectra, and restricting the analysis to higher temperatures. A relaxation time can be defined from the frequency of the maximum in the loss, $\tau = (2\pi f_{max})^{-1}$, and these are plotted in Figure 7 as a function of the specific volume. The dynamics in the cholesteric phase is sensitive to both temperature and pressure; hence, the isobaric and isothermal curves have different slopes.

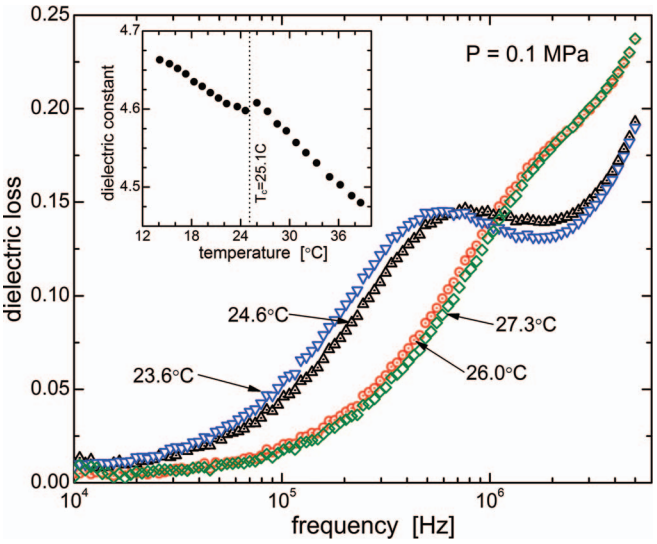

FIG. 5. Dielectric spectra measured ambient pressure for the cholesteric phase (triangles and inverted triangles) and the isotropic liquid (circles and diamonds); only the former exhibits a relaxation peak. The inset shows the in-phase component of the relative permittivity at various temperatures traversing the isotropic-cholesteric transition.

The dependence of relaxation times and other dynamic variables (e.g., diffusion constant or viscosity) has been shown to be uniquely defined by the product variable in Eq. (1).[6–8] The cholesteric phase τ are plotted accordingly in

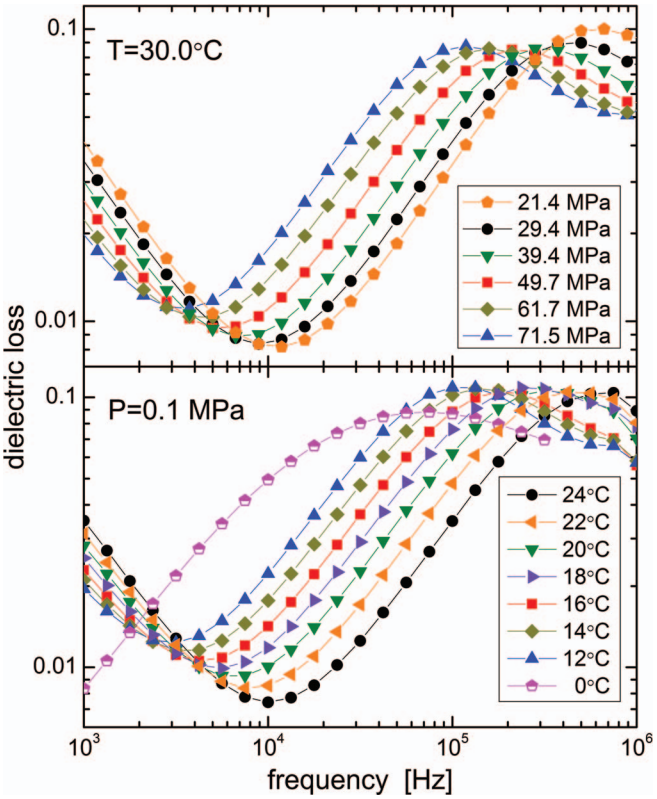

FIG. 6. Dielectric relaxation spectra for the cholesteric phase (top) at the indicated pressures at 30 °C and (bottom) at the indicated temperatures at ambient pressure. The lines are only to guide the eyes; the peaks are slightly broader than Debye (FWHM > 1.14 decades). The rise at lower frequencies is due to ionic conductivity. For the lowest temperature (half-filled pentagons), the sample is crystallizing, which distorts the spectral shape.

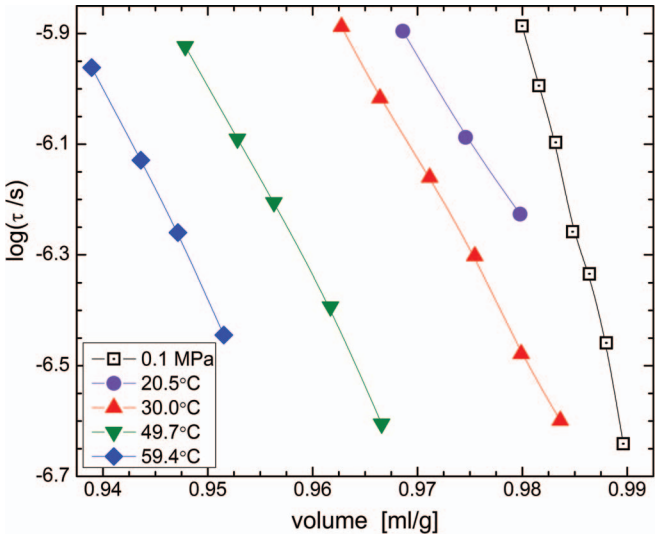

FIG. 7. Relaxation times for the cholesteric phase as a function of specific volume. Note the different dependences for varying pressure versus varying temperature.

Figure 8, with the exponent, $\gamma = 3.5 \pm 0.2$, determined by adjusting its value to optimize the superpositioning of the data. The large uncertainty reflects the approximate conformance to this scaling property, although some of the scatter in the data is due to uncertainty in resolving the loss peak at higher frequencies involving reorientation about the long axis of the molecule; the separation of the two dispersions changes with T and P (see Fig. 7).

An equation derived from an entropy formulation of the glass transition has been proposed to describe the scaling property[23]

$$\tau = \tau_0 \exp\left[\left(\frac{A}{TV^{\gamma}}\right)^{\phi}\right] \tag{6}$$

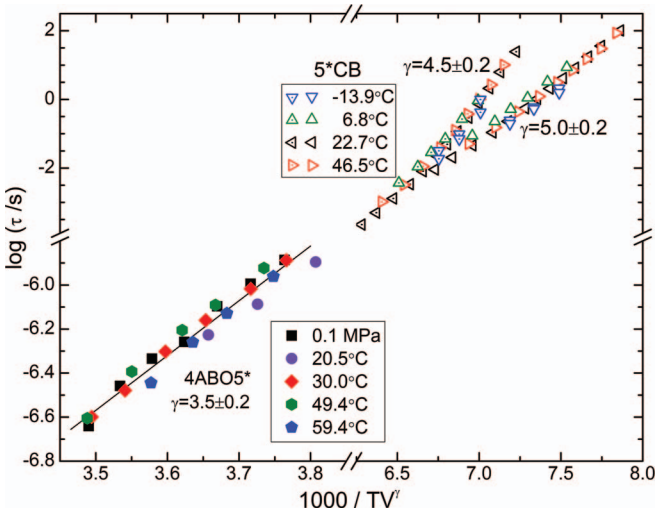

FIG. 8. Scaling plots for two cholesteric liquid crystals: 4ABO5* (filled symbols) and isopentylcyanobiphenyl (open and dotted symbols),[19] the latter having two relaxations. The superpositioning is mediocre, with the best values of the scaling exponent as indicated. The solid line is the fit of Eq. (6) to the 4ABO5* data.

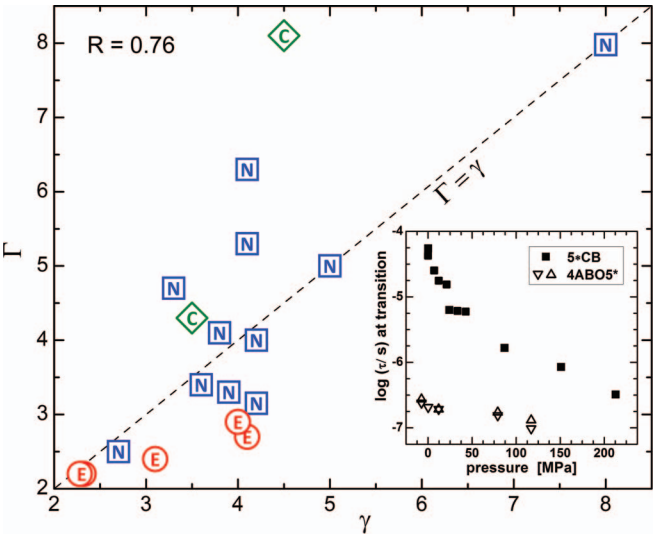

FIG. 9. Thermodynamic ratio versus the dynamic scaling exponent for 18 liquid crystals; N = nematic, C = cholesteric, E = smectic E. The highest datum ($\Gamma = \gamma = 8$) corresponds to the result from mds.[15] The inset compares the relaxation times at the clearing point for 5*CB (squares)[19,20] and 4ABO5* determined by extrapolation of τ versus P (triangles) and versus V (down triangles).

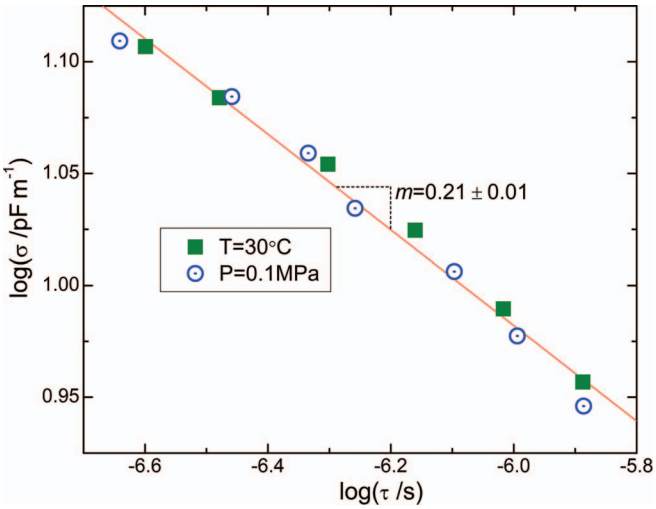

FIG. 10. Ionic conductivity versus the relaxation time for 4ABO5* in the cholesteric state.

in which τ_α, A, and ϕ are material constants. This equation describes accurately relaxation times for many supercooled liquids, with ϕ in the range from 2–8.[24] For 4ABO5* log τ is a linear function of $T^{-1}V^{-\gamma}$, so that the $\phi = 1$. Although this could be due to the limited range over which the cholesteric state is stable, another liquid crystal, isopentylcyanobiphenyl (5*CB), which has two relaxations in the dielectric spectrum for the cholesteric state,[19] shows the same behavior (Fig. 8). Linearity in these Arrhenius-type plots is consistent with thermally activated dynamics and an activation energy that has a volume-dependence described by V^γ. This is not the case for supercooled, isotropic liquids, for which τ_α vs. TV^γ plots exhibit marked curvature.[8,25]

If the relaxation time is constant at a phase transition, it follows from Eqs. (1) and (3) that $\Gamma = \gamma$.[6,13] In Figure 9 these two parameters are plotted for various liquid crystals, including nematics, smectics, and cholesterics. The general correlation is poor (Pearson's coefficient < 0.8). For the 4ABO5* $\Gamma = 4.3$ and $\gamma = 3.5$. For 5*CB, another chiral liquid crystal, there is no correspondence, $\Gamma = 8.1$ and $\gamma = 4.5$. Constancy of the relaxation time at the clearing point follows from $\Gamma = \gamma$, and as seen in the inset to Fig. 9, the variation of τ with pressure for 4ABO5* is much less than for 5*CB. The latter material has a monotropic cholesteric phase (chiral phase is below the melting temperature of the crystalline solid phase).[19] The volume change at the clearing line, always small for cholesterics, is almost negligible for 5*CB, which amplifies any influence of crystallization. 5*CB is also very polar (dipole moment of the CN group is 4.05 D), with strong antiparallel association between molecules and an equilibrium between monomeric and dimeric forms. The concentration of dimers increases with increasing T,[26] and since they are ~40% longer than the molecular length,[27] this dimer concentration affects the volume at the pressure-dependent clearing point.

Finally, we note that for isotropic liquids the dc ionic conductivity, σ, is coupled to the structural relaxation, molecular reorientation serving as the mechanism to open diffusive pathways. An empirical power law, a generalization of the Debye-Stokes-Einstein equation,

$$\sigma\tau^m = \text{const.}, \tag{7}$$

is commonly used to describe the coupling of ionic conduction and dielectric relaxation,[28] with the exponent having values in the range $0 < m < 1$. This relation assumes the number of charge carriers is constant. In Figure 10 the dc-conductivity is plotted versus the relaxation time for 4ABO5* in the cholesteric phase. Their correlation is evident, and it is the same for varying temperature as for varying pressure.

IV. SUMMARY

From PVT and dielectric relaxation measurements, the relationship between the thermodynamic behavior and the dynamics in the cholesteric phase of a newly synthesized chiral nematic liquid crystal was examined. Two parameters characterizing the steepness of the intermolecular potential were determined: the thermodynamic potential parameter (Eq. (3)) and the dynamic scaling exponent (Eq. (6)). The difference between them, $\Gamma = 4.3 \pm 0.1$ and $\gamma = 3.5 \pm 0.2$, is similar to that found for many nematic liquid crystals, as illustrated in Fig. 9. The near equivalence for 4ABO5* indicates that the time constant for reorientation is roughly constant along the clearing line, as verified by extrapolation of the measured τ.

ACKNOWLEDGMENTS

The work at NRL was supported by the Office of Naval Research. D.R. acknowledges a Naval Research Laboratory/National Research Council postdoctoral fellowship.

[1] *Handbook of Liquid Crystals*, edited by D. Demus, J. Goodby, G. W. Gray, H. W. Spiess, and V. Vill (Wiley-VCH, Weinheim, 1998).
[2] S. Chandrasekhar, *Liquid Crystals*, 2nd ed. (Cambridge University Press, New York, 1992).

[3]S. Singh, Phys. Rep. **324**, 107–269 (2000).
[4]W. Maier and A. Saupe, Z. Naturforsch. **14a**, 882–889 (1959); **15a**, 287–292 (1960); **1961**(16a), 816–824 (1961).
[5]L. Onsager, Ann. N.Y. Acad. Sci. **51**, 627–659 (1949).
[6]S. Urban, Liq. Crystallogr. **38**, 1147–1152 (2011).
[7]C. M. Roland, R. B. Bogoslovov, R. Casalini, A. R. Ellis, S. Bair, S. J. Rzoska, K. Czuprynski, and S. Urban, J. Chem. Phys. **128**, 224506 (2008).
[8]C. M. Roland, *Viscoelastic Behavior of Rubbery Materials* (Oxford University Press, 2011).
[9]D. Coslovich and C. M. Roland, J. Phys. Chem. B **112**, 1329–1332 (2008).
[10]U. R. Pedersen, T. B. Schrøder, and J. C. Dyre, Phys. Rev. Lett. **105**, 157801 (2010).
[11]J. R. McColl and C. S. Shih, Phys. Rev. Lett. **29**, 85–87 (1972).
[12]J. R. McColl, Phys. Lett. A **38**, 55–57 (1972).
[13]S. Urban and C. M. Roland, J. Non-Cryst. Solids **357**, 740–745 (2011).
[14]C. M. Roland, D. Fragiadakis, R. Bogoslovov, S. Urban, R. Dabrowski, M. Tykarska, N. Osiecka, and J. Czub, Liq. Crystallogr. **39**, 993–1001 (2012).
[15]K. Satoh, J. Chem. Phys. **138**, 094903 (2013); **139**, 084901 (2013).
[16]C. M. Roland, Soft Matter **4**, 2316–2322 (2008).
[17]D. Ben-Amotz and G. J. Stell, J. Chem. Phys. **119**, 10777–10788 (2003).
[18]N. P. Bailey, U. P. Pedersen, N. Gnan, T. B. Schrøder, and J. C. Dyre, J. Chem. Phys. **129**, 184508 (2008).
[19]D. Fragiadakis, S. Urban, M. Massalska-Arodz, R. B. Bogoslovov, J. Czub, and C. M. Roland, J. Phys. Chem. B **115**, 6437–6444 (2011).
[20]S. J. Rzoska, M. Paluch, S. Pawlus, A. Drozd-Rzoska, J. Ziozo, J. Jadzyn, K. Czupryński, and R. Dabrowski, Phys. Rev. E **68**, 031705 (2003).
[21]R. Dąbrowski, G. Adamska, Z. Stolarzowa, and A. Konarzewski, Polish J. Chem. **54**, 1233–1234 (1980).
[22]P. Zoller and D. J. Walsh, *Standard Pressure–Volume–Temperature Data for Polymers* (Technomic Publications, Lancaster, PA, 1995).
[23]R. Casalini, U. Mohanty, and C. M. Roland, J. Chem. Phys. **125**, 014505 (2006).
[24]R. Casalini and C. M. Roland, J. Non-Cryst. Solids **353**, 3936–3939 (2007).
[25]C. M. Roland, S. Hensel-Bielowka, M. Paluch, and R. Casalini, Rep. Prog. Phys. **68**, 1405–1478 (2005).
[26]M. Brodzik, R. Dąbrowski, and J. Przedmojski, J. Phys. II France **5**, 1805–1817 (1995)
[27]A. J. Leadbetter, J. C. Frost, J. P. Gaughan, G. W. Gray, and A. Mosley, J. Phys. France **40**, 375–380 (1979)
[28]H. Sasabe and S. Saito, Polym. J. (Tokyo) **3**, 624–630 (1972).